ACS OMEGA

Open Access

http://pubs.acs.org/journal/acsodf

Article

Numerical Investigation of Hydrogen-Blended Low-Calorific-Value Landfill Gas Combustion: Flame Stability and Pollutant Suppression in Porous Media Burners

Kang Tan, Udaya Kahangamage,* Kangdong Chen, and Chun-wah Leung

Cite This: *ACS Omega* 2025, 10, 41809−41819

Read Online

ACCESS | Metrics & More | Article Recommendations

ABSTRACT: This study investigates the combustion characteristics of hydrogen-enriched low-calorific landfill gas (LFG) in a double-layer porous media burner by using numerical simulations. The research addresses challenges related to flame instability and pollutant emissions during low-calorific LFG combustion. A two-dimensional axisymmetric numerical model was developed in ANSYS Fluent, incorporating a skeletal chemical reaction mechanism and the standard k-ε turbulence model. Simulations were performed with LFG composed of 30% methane and 70% carbon dioxide (LFG30) under varying hydrogen blending ratios (0 to 20%), an equivalence ratio of 1.5, and an inlet gas velocity of 0.15 m/s. The results demonstrate that increasing hydrogen concentrations shifts the flame upstream, lowers both combustion and exhaust gas temperatures, and significantly decreases CO and NO_x emissions. When the hydrogen blending ratio reaches 20%, the mole fractions of CO and NO_x at the outlet are reduced by 22.14 and 72.65%, respectively, compared with the pure LFG30. The findings indicate that hydrogen enrichment significantly enhances the combustion stability and emission performance of low-calorific LFG in porous media burners, providing an effective approach for efficiently utilizing low-calorific-value fuels even at extreme operating conditions. This study offers novel insights toward the development of effective burners aimed at increasing the utilization of this underutilized renewable energy resource and addressing environmental concerns.

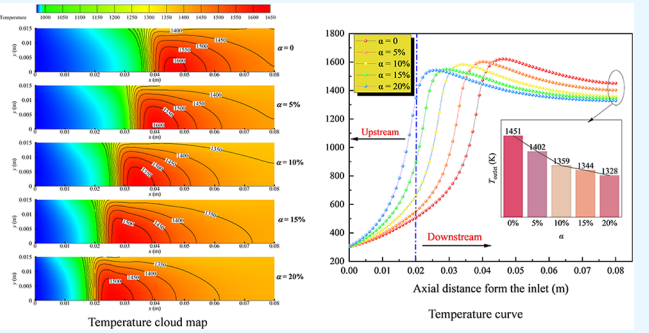

1. INTRODUCTION

Over the last few decades, the world has experienced rapid urbanization and industrialization, which have led to two of the most pressing challenges faced by modern society: environmental pollution and resource depletion.[1] To address the critical issues of energy scarcity and environmental degradation, the development and efficient utilization of clean and sustainable energy sources have become essential.[2] One such renewable energy resource is landfill gas (LFG), which is generated through the anaerobic decomposition of solid waste produced by both industrial activities and daily human activities. Due to its abundance, widespread availability, and simple production process, LFG is regarded as an energy source with significant potential for applications. However, the primary components of LFG, methane (CH_4) and carbon dioxide (CO_2), are potent greenhouse gases that contribute to global warming. Notably, the global warming potential (GWP) of methane is 28−36 times higher than that of CO_2.[3] Consequently, the direct release of LFG into the atmosphere not only exacerbates environmental issues but also results in a substantial loss of a valuable renewable energy resource. Technological innovation and advancement are necessary to better harness the energy content of LFG. Among the available solutions, combustion technology offers a feasible approach for the effective utilization of LFG. Over the past three decades, LFG combustion-based power generation has become one of the widely adopted methods in many developed countries,[4] as it helps reduce greenhouse gas emissions and due to its cost effectiveness.[5] Moreover, LFG has been extensively used in residential heating and automotive engines. LFG containing a high concentration of methane (CH_4 > 40%) is utilized in various industrial applications. In contrast, LFG with lower methane content (CH_4 < 40%) is typically managed through onsite flaring or direct emission to the atmosphere, contributing to greenhouse gas emissions.[6]

LFG is characterized by low heating value, unstable combustion, ignition difficulties, sensitivity to flow rate, and

Received: June 18, 2025
Revised: August 21, 2025
Accepted: September 1, 2025
Published: September 4, 2025

a high tendency to extinguish, which makes it challenging for conventional combustion technologies to use efficiently. On the other hand, porous media combustion (PMC) technology offers significant advantages, such as stabilizing the combustion flame, preheating the upstream fuel mixture, and achieving a uniform temperature distribution within the combustion chamber.[7,8] These characteristics are highly beneficial for the efficient combustion and utilization of LFG. Currently, PMC technology has been widely applied in various applications, including household stoves,[9] thermophotovoltaic power generation,[10] and internal combustion engines.[11] The strong thermal recirculation in porous media can make otherwise nonflammable fuel mixtures combustible, enhance flame stability, and reduce pollutant emissions.[12,13]

Effective burner design can enhance the utilization efficiency of low-calorific-value fuels. A two-layer design with significantly different porosities is more effective in maintaining flame stability, a concept that has been reported in previous studies.[14−16] In two-layer porous burners, a porous medium with lower thermal conductivity and porosity is typically placed in the upstream area near the burner inlet, while a porous medium with higher thermal conductivity and porosity is positioned in the downstream area. This arrangement allows the downstream porous medium to transfer heat upstream, preheating the fresh fuel-air mixture. The thermal equilibrium established by the two layers of porous media, each with different properties, tends to stabilize the flame at the interface, thereby reducing the risk of flashback.[17] Devi et al.[18] developed a testing platform for raw biogas combustion using a circular double-layer porous radiant burner made of silicon carbide and alumina. They investigated the effects of input power and equivalence ratio on combustion characteristics, finding that the thermal distribution across the burner was uniform under all of the tested conditions. Chen et al.[14] conducted a numerical investigation into the influence of pore size gradients and porosity gradients on the combustion characteristics and flame stability of hydrogen-enriched natural gas. The study found that within axially graded porous structures, increasing the pore size led to an approximately 26% rise in the maximum temperature. Bubnovich et al.[19] investigated the combustion of propane-air mixtures in double-layer porous media burners constructed from three types of porous ceramics: reticulated alumina foam, honeycomb alumina foam, and silicon carbide foam. They experimentally analyzed CO and NO_x emissions and thermal characteristics, finding that the flame stabilized between the two layers of porous ceramics, with CO and NO_x emissions remaining very low. Habib et al.[20] tested the stability of methane-hydrogen mixtures under oscillating hydrogen concentrations in double-layer porous media and found that porous media significantly promoted flame stability. Keramiotis et al.[21] used a mixture of 60% CH_4 and 40% CO_2 to simulate typical biogas fuel and investigated the combustion stability and emission performance (NO_x and CO) of biogas in a rectangular double-layer porous media burner. The results indicated that the physical effects of CO_2 were more significant than its chemical effects, resulting in lower CO and NO_x emissions.

Alongside porous media combustion technology, fuel blending has been studied as a method for improving the combustion performance of low-calorific-value fuels. Kahangamage and Chen[6,22] used numerical models to study hydrogen-rich combustion of LFG with less than 40 vol % CH_4. They found that adding hydrogen increases laminar burning velocity, and the mixed fuel composed of LFG with 30 vol % CH_4 and 30 vol % hydrogen matches 60 vol % CH_4 biogas in heat transfer intensity. They also noted that the combustion performance improved further under fuel-rich conditions. Francisco et al.,[23] using a laboratory-scale burner, investigated the flame stability and pollutant emissions of $CH_4/CO/H_2$ low-calorific-value gas mixtures diluted with CO_2 and N_2 in porous media. The results indicated that similar to free flames, the increased hydrogen concentration in the mixture significantly expanded the stable operating range of the burner. Amez et al.[24] studied biogas-H_2 blends in a standard combustion system, testing rich (70% CH_4), standard (60% CH_4), and poor (50% CH_4) biogas with up to 20% H_2. Improvements in flame stability were most notable between 5 and 10% hydrogen, with standard and rich biogas at 10% H_2 producing flame structures similar to natural gas. However, flame temperatures remained below those of natural gas.

The integration of porous media with hydrogen addition results in a system that demonstrates enhanced stability, improved efficiency, and potential for cleaner operation compared to the use of either technology independently. Chen et al.[25] investigated the synergistic effect of porous media combustion and hydrogen doping on the combustion of natural gas in domestic water heaters. The results show that the combination of porous media and hydrogen doping led to a more complete combustion and lower pollutant emissions. Tolouei et al.[26] studied the effect of hydrogen enrichment and catalytic porous media on the combustion characteristics of CH_4/NH_3 gas mixtures. The combined effect of catalytic porous media and hydrogen enrichment has resulted in low-emission and efficient combustion. The study additionally demonstrated that the combined use of hydrogen and inert porous media resulted in approximately 87% lower NO_x emissions compared to free flame combustion, with an additional 59% reduction observed when catalytic porous media was used.

The literature reviewed indicates that numerous studies have examined the combustion performance of hydrogen-enriched methane and biogas within inert or catalytic porous media. However, there is a paucity of research concerning the application of hydrogen enrichment and porous media combustion for the utilization of landfill-derived low-calorific gases, which are often flared onsite or released directly into the atmosphere, thereby contributing to environmental concerns. By exploring the combined benefits of hydrogen enrichment and porous media combustion for low-calorific landfill gases, this research offers novel insights toward the development of effective burners and promoting the utilization of this underutilized renewable energy resource with potential environmental benefits. In this study, a two-dimensional axisymmetric numerical model based on a widely used double-layer porous ceramic foam burner[27] was used to perform a detailed investigation of hydrogen-enriched low-calorific LFG. Analyses were conducted to investigate the temperature distribution, combustion chemical reaction structure, and chemical reaction sensitivities within the porous media burner under conditions where hydrogen concentrations in low-calorific LFG ranged from 0 to 20%. The LFG, composed of 30% CH_4 and 70% CO_2 (LFG30), considered in this study, is characterized by a low-calorific value and a high content of inert gas. Under fuel-rich conditions ($\Phi > 1$), the oxygen deficiency exacerbates incomplete combustion, leading to elevated CO emissions and flame instability.[21] By examining

https://doi.org/10.1021/acsomega.5c05809
ACS Omega 2025, 10, 41809−41819

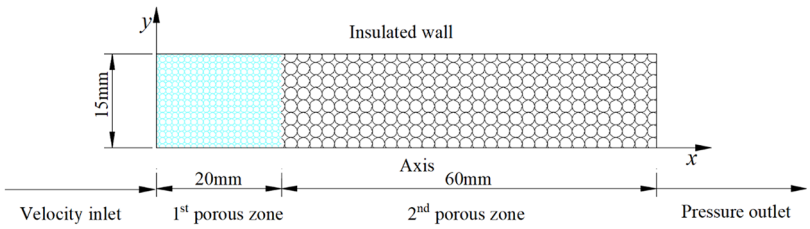

Figure 1. Geometric model and boundary conditions of the porous media burner.

combustion characteristics for Φ = 1.5, this work intentionally magnifies these challenges, thereby providing a stringent testbed to evaluate the effectiveness of hydrogen blending in mitigating such issues.

2. NUMERICAL MODEL AND SIMULATION METHOD

2.1. Geometric Model. In this study, a two-layer porous media geometric model was established using ANSYS ICEM software, based on the experimental setup from Wang et al.[27] as shown in the Figure 1. The model consists of two porous zones with significantly different pore sizes. The combustor has a total length of 80 mm and a radius of 15 mm. The upstream section (depicted in light blue) has an average pore size of 0.75 mm and a porosity of 0.40, while the downstream section has an average pore size of 2.34 mm and a porosity of 0.45. Both porous media regions are made of an Al_2O_3 foam structure. The boundary conditions of the combustor wall are set as adiabatic, and heat loss is not considered. Detailed material properties are listed in Table 1. The combustion process in porous media involves the coupling effects of flow, chemical reactions, heat transfer, and radiation, which form the core mechanism of the system.

Table 1. Summary of the Key Simulation Parameters Used for Numerical Investigations

parameter	value
inlet mixture velocity, u_{in} (m/s)	0.15
ambient pressure (kPa)	101
unburned mixture temperature (K)	300
landfill gas composition	30%CH_4+70%CO_2
equivalence ratio (Φ)	1.5
blending ratio of H_2 (α)	0−20%
porosity of 1st porous zone	0.4 (pore diameter 0.75 mm)
porosity of 2nd porous zone	0.45 (pore diameter 2.34 mm)
thermal conductivity of Al_2O_3 (W/m K)	400
specific thermal capacity of Al_2O_3 (J/kg)	0.77

2.2. Mathematical Model. In order to save computing resources and reduce computing time, this study simplifies the three-dimensional axisymmetric model into a two-dimensional axisymmetric model. The following assumptions are also made:

(1) Mixed gas is a completely mixed and uniform incompressible ideal gas.
(2) The porous medium is inert and isotropic.[6]
(3) The radiation effect and buoyancy effect of the gas phase are ignored.[28]
(4) It is assumed that the gas phase and the solid phase are in thermal equilibrium.
(5) Gas flow, heat conduction, and convective heat transfer between the gas and solid phases are assumed to be two-dimensional.
(6) The combustion model ignores the influence of the Dufour effect.

Given these assumptions, the conservation equations are as follows:

Continuity equation:

$$\nabla(\varepsilon\rho_g\vec{u}) = 0 \tag{1}$$

where ε is the porosity of the porous medium, and ρ_g is the density of the fuel/air mixture.

Momentum equation:

Momentum equation in the x direction:

$$\nabla(\varepsilon\rho_g u\vec{u}) = -\frac{\partial p}{\partial x} + \nabla(\mu\nabla u) + \frac{\mu}{C_1}u + \frac{\rho_g}{C_2}u^2 \tag{2}$$

Momentum equation in the y direction:

$$\nabla(\varepsilon\rho_g v\vec{v}) = -\frac{\partial p}{\partial y} + \nabla(\mu\nabla u) + \frac{\mu}{C_1}v + \frac{\rho_g}{C_2}v^2 \tag{3}$$

where C_1 and C_2 are the viscous resistance coefficient and inertial resistance coefficient of porous ceramics, respectively.

Energy equation:

$$\nabla(\varepsilon\rho_g v\vec{u}) = \lambda_{eff}\nabla T - \sum_i h_i\omega_i W_i \tag{4}$$

where λ_{eff} represents the effective thermal conductivity of the porous medium, and its value can be calculated by the following expression:

$$\lambda_{eff} = \varepsilon\lambda_g + (1-\varepsilon\lambda_s) \tag{5}$$

where λ_g is the thermal conductivity of the gas phase, and λ_s is the thermal conductivity of the solid phase.

Species conservation equation:

$$\nabla(\varepsilon\rho_g\vec{u}Y_i) = \nabla[\varepsilon D_{in}\nabla(\rho Y_i)] + \varepsilon\omega_i W_i \tag{6}$$

In the formula, Y_i represents the local mass fraction of species i, D_{in} is the mass diffusion coefficient of species i, ω_i is the molar yield of species i, and W_i is the relative molecular mass of species i.

Ideal gas equation:

$$P = \frac{\rho RT}{\bar{W}} \tag{7}$$

where, $\bar{W}$ is the average molecular weight of the mixed gas.

The blending ratio of hydrogen in the mixture α is defined as

$$\alpha = \frac{n_{H_2}}{n_{H_2} + n_{LFG}}\% \tag{8}$$

2.3. Mesh Independence Check. Mesh independence verification is a critical step in simulation analysis to evaluate

https://doi.org/10.1021/acsomega.5c05809
ACS Omega 2025, 10, 41809−41819

the stability and accuracy of the numerical model under different mesh resolutions.[29] Variations in mesh resolution can significantly influence the numerical results. Generally, higher mesh resolution leads to more accurate results; however, it also increases the computational time and memory requirements. Therefore, conducting mesh independence analysis allows for the assessment of solution variations under different mesh densities, enabling the selection of a numerical model that accurately reflects physical behavior while maintaining computational efficiency. Figure 2 illustrates the simulation

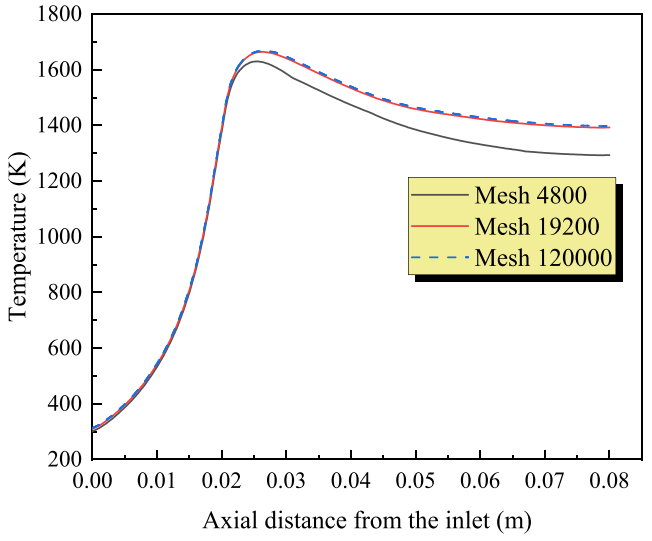

Figure 2. Comparison of axial temperature distribution of the porous burner by using three different mesh resolutions (u_{in} = 0.15 m/s and Φ = 1.5 for CO_2/CH_4 = 1.0).

results obtained for the temperature distribution along the axis of the combustion chamber for three mesh resolutions. To accurately capture the steep temperature gradient and significant variations of reacting species within the narrow combustion zone, the mesh has been locally refined in this region for each case, relative to other areas. Each scenario underwent more than 200,000 iterations, and the residual of the continuity equation reduced to 1.0×10^{-6}, meeting the required accuracy criteria. Although all three mesh resolutions exhibit similar trends, the results for mesh size of 19,200 are nearly identical to those for the mesh size of 120,000. In contrast, the results for mesh size of 4800 show significant deviations from the other two. Consequently, to balance computational accuracy and efficiency, this study adopts a mesh size of 19,200 for the simulation analysis.

2.4. Boundary Conditions and Solutions. ANSYS FLUENT 2022R1 was used to solve the 2D numerical model constructed above. The burner outlet and inlet were set as velocity inlet and pressure outlet with an initial temperature and pressure of 300 K and 101 kPa, respectively. The thermophysical properties and diffusion characteristics of the mixed gas at the inlet were determined using the CHEMKIN database. For the gas phase combustion reaction mechanism, this study adopted a skeletal mechanism consisting of 16 species and 41 reactions.[30] Prior research has shown that this mechanism is capable of obtaining accurate results in predicting the thermal characteristics of methane-air laminar combustion. Furthermore, Wei et al.[10] compared the experimental and numerical simulation results, demonstrating the effectiveness of this mechanism in predicting the thermal and emission characteristics of methane-hydrogen combustion. In this paper, the standard k-ε turbulence model was used to calculate the turbulent viscosity in the control equation more accurately.[31] The pressure and velocity were coupled and interconnected by the SIMPLE algorithm.[32] In addition, to make the numerical calculation results more accurate, the second-order upwind scheme is used to discretize and solve the convection terms in the momentum equation and energy equation. The convergence of the calculation model is defined here as when the residual of the discrete continuity equation drops to 1.0×10^{-6} and the other equations (mass, momentum, species) drop to 1.0×10^{-3}. The ignition process is achieved by setting the initial temperature of the entire calculation domain.

2.5. Numerical Model Validation. To validate the accuracy and reliability of the numerical model developed in this study, numerical simulation results were compared with the experimental temperature distribution reported by Zeng et al.[33] under identical operating conditions. Specifically, the comparison was conducted for a mixture flow velocity of u_{in} = 0.15 m/s, an equivalence ratio of Φ = 1.5, and a landfill gas composition with a methane-to-carbon dioxide ratio of CO_2/CH_4 = 1.0. The comparison is shown in Figure 3. The figure

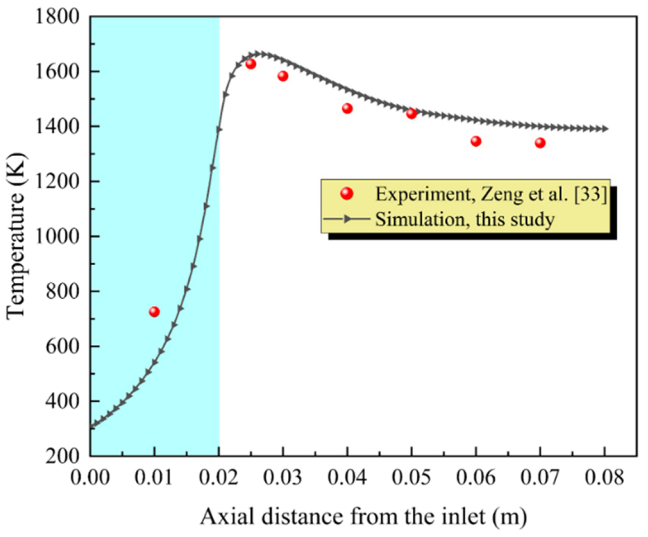

Figure 3. Comparison of axial temperature distribution of simulation results and experiment data at u_{in} = 0.15m/s and Φ = 1.5 for CO_2/CH_4 = 1.0. Reprinted with permission from ref 33 Copyright 2017 Elsevier.

illustrates the axial temperature distribution trend during CH_4/CO_2/air premixed combustion. As observed, both the experimental data and the numerical results exhibit a similar trend, where the axial temperature first increases and then decreases, with the peak temperature occurring near the interface between the upstream and downstream regions. Furthermore, the maximum relative error between the numerical results and the experimental data is less than 5%, which is within an acceptable range for the present model. Therefore, the proposed model is considered suitable for studying hydrogen-enriched combustion of landfill gas.

The numerical model validation described above utilized experimental data available for LFG composition with a methane-to-carbon dioxide ratio of CO_2/CH_4 = 1.0. However,

https://doi.org/10.1021/acsomega.5c05809
ACS Omega 2025, 10, 41809−41819

the fuel blends investigated in this study consisted of LFG with 30% CH_4. To the best of our knowledge, no publicly available experimental data exist for LFG with 30% CH_4 that is suitable for model validation. Given that both fuel mixtures contain the same gases and relatively high concentrations of inert gas (CO_2), it is assumed that the variation in fuel composition has a minimal influence on model behavior.

3. RESULTS AND DISCUSSIONS

In general, LFG is composed of methane, carbon dioxide, and a small amount of other organic compounds.[34] The other trace components are ignored in this study, and 30% methane and 70% CO_2 (LFG30) are used to simulate low-calorific value LFG.

3.1. Effect of Hydrogen Blending Ratio in the Inlet LFG30 Mixture on the Flame Stability. In double-layer porous media burners, the stable combustion range is conventionally defined by identifying the flow velocities that produce an anchored flame near the two extreme ends of the combustion zone. This indicates the existence of a minimum stable velocity for flame propagation, which marks the transition threshold between flame stability and flashback; as well as a maximum stable velocity that defines the boundary between sustained combustion and flame blow-off.[35] Figure 4 illustrates the upper and lower velocity limits under various hydrogen blending ratios.

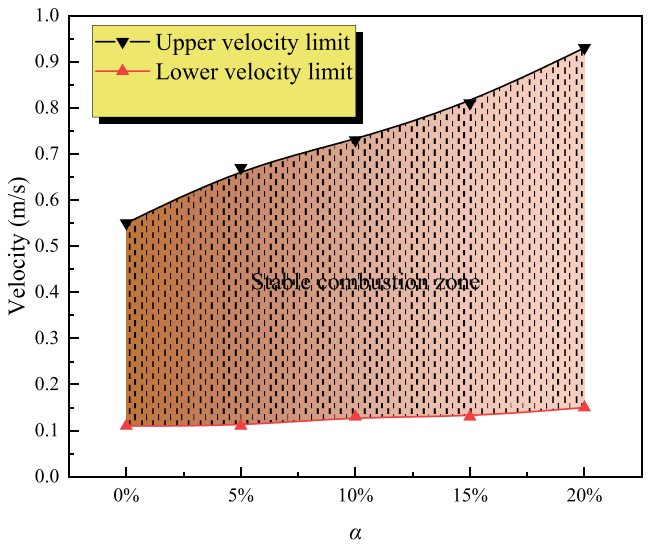

Figure 4. Effect of hydrogen blending ratio in the LFG30 mixture on the stable combustion zone at Φ = 1.5.

As the hydrogen blending ratio increases, the stable combustion range progressively widens. The lower velocity limit exhibits negligible variation, remaining within 0.11 to 0.15 m/s, while the upper limit shows marked enhancement. When hydrogen is gradually blended into LFG30, its high thermal diffusivity accelerates the upstream heat recirculation through the porous matrix. The resulting preheating effect on unburned mixtures elevates the local burning velocity. When the burning velocity increases, blow-off is suppressed, and the operable inlet flow velocity range expands. Increased hydrogen content not only shifts the flame front upstream but also prolongs the residence time within the porous media, enabling continuous preheating of fresh mixtures by combustion heat. However, when the inlet velocity drops below the burning velocity, the flame migrates toward the burner base, inducing flashback risks. This broadening of the stable combustion range with the addition of hydrogen substantially enhances operational flexibility. As a critical parameter for burner stability, it provides a scientific theoretical foundation for selecting and designing operating regimes for low-calorific-value fuel utilization systems.

3.2. Effect of Hydrogen Blending Ratio on Temperature Distribution in the Burner. Figure 5 shows the two-dimensional temperature distribution in the burner with an inlet gas velocity (u_{in}) of 0.15 m/s and an equivalence ratio (Φ) of 1.5. The figure shows that as the hydrogen concentration in the mixed fuel increases, the overall temperature downstream of the burner decreases. Additionally, the area enclosed by 1600 K temperature contour shrinks with higher hydrogen ratios, indicating a downward temperature trend inside the porous media burner.

Under standard pressure and temperature conditions, the volumetric heat value of methane is 35.88 MJ/m^3, while that of hydrogen is 10.78 MJ/m^3. Consequently, when the hydrogen proportion increases from 0 to 20%, the volumetric heat value of the mixed fuel increases from 9.860 to 9.866 MJ/m^3. This indicates that hydrogen blending does not significantly affect the volumetric heating value, so the heat release per unit volume will not change significantly. At the same time, the addition of hydrogen increases the average specific heat capacity of the inlet mixed fuel from 1030.6 J/(kg· K) to 1216.2 J/(kg· K). Therefore, to achieve the same flame temperature, more heat generation is required. However, the addition of hydrogen significantly affects the concentrations of related radicals in the radical pool, thereby influencing the chain branching reactions in the combustion process to varying degrees, which indirectly leads to changes in the burner internal temperature. From the perspective of radial temperature variations, the temperature change at the same radial position ranges between 150−200 K.

To provide a more intuitive analysis of the temperature distribution inside the burner, the axial temperature profiles under different hydrogen concentrations were compared, as shown in Figure 6. With the increase in the hydrogen molar fraction, the downstream axial temperature in the burner gradually decreases, which aligns with the computational results obtained from the temperature contour plots. Furthermore, based on the outlet temperatures displayed in the histogram given in Figure 6, it can be observed that when the hydrogen molar fraction increases from 0 to 20% with 5% increments, the outlet temperatures decrease by 49, 43, 15, and 16 K, respectively. However, the upstream temperature increases with the increase of the hydrogen mole fraction, and the axial temperature gradually increases. This is due to the high thermal diffusivity of hydrogen, which accelerates the combustion rate, and the high-temperature area of the flame shifts upstream. At the same time, in combination with the good heat absorption capacity of the porous medium, the heat dissipation via emissions is reduced. Therefore, adding hydrogen to landfill gas in a porous medium burner can effectively reduce the exhaust gas temperature and improve the overall performance of the burner.

The peak temperature is an important parameter for describing the combustion characteristics of a landfill gas. This study analyzed the effects of different hydrogen concentrations added to landfill gas on the magnitude and position of the peak flame temperature, as shown in Figure 7. It

https://doi.org/10.1021/acsomega.5c05809
ACS Omega 2025, 10, 41809−41819

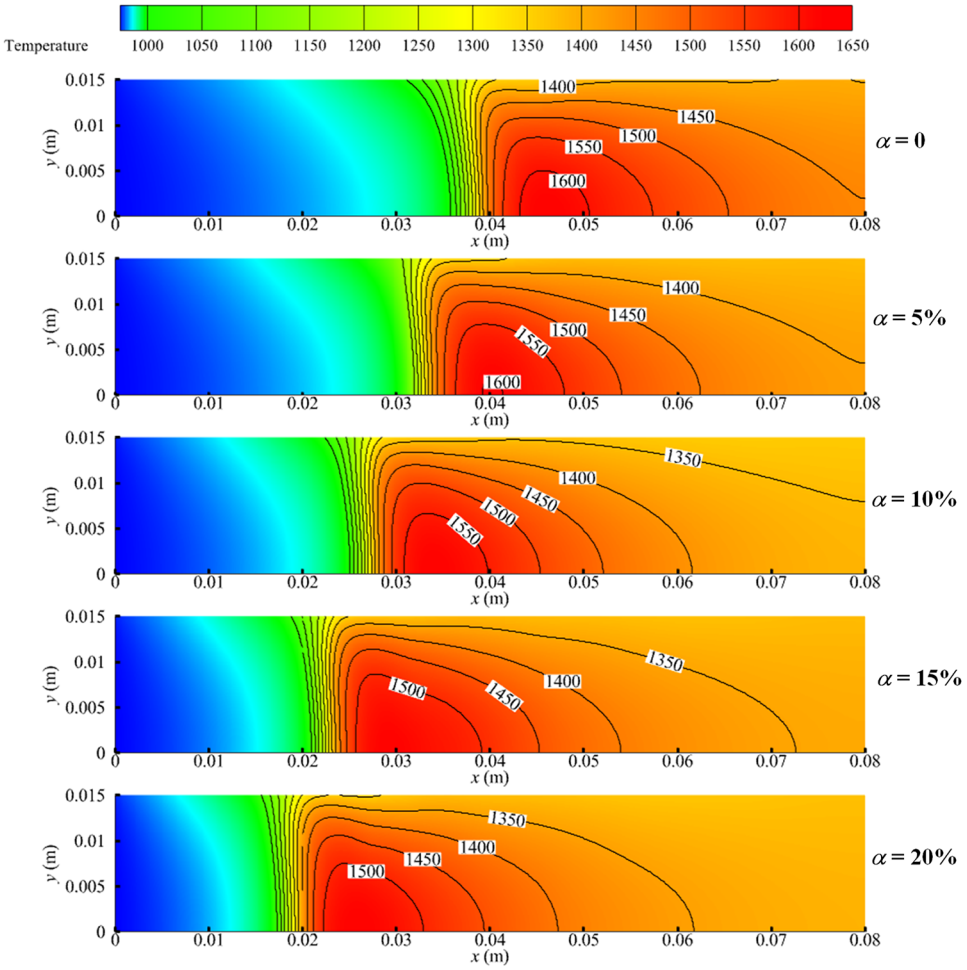

Figure 5. Effect of hydrogen blending ratio in the LFG30 mixture on two-dimensional temperature distribution in the burner at flow velocity, u_{in} = 0.15 m/s and Φ = 1.5.

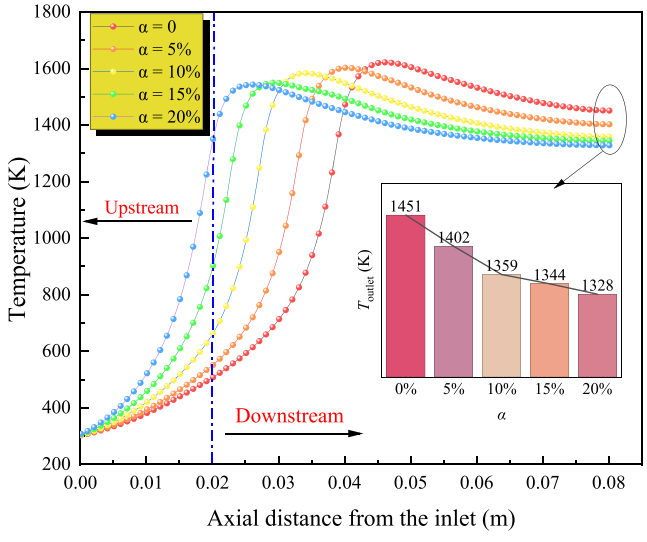

Figure 6. Effect of hydrogen blending ratio (α) in the LFG30 mixture on axial temperature distribution at flow velocity, u_{in} = 0.15 m/s and Φ = 1.5.

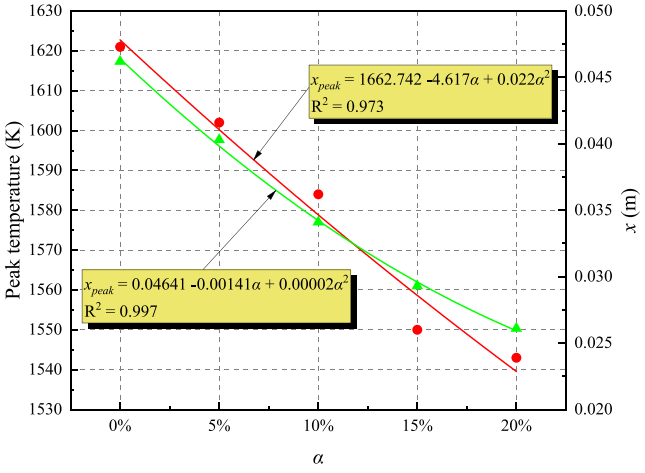

Figure 7. Effect of hydrogen blending ratio in the LFG30 mixture on peak temperature value and its axial positions at flow velocity, u_{in} = 0.15 m/s and Φ = 1.5.

can be observed that increasing the hydrogen molar fraction decreases the peak flame temperature. The relationship follows a quadratic function with a negative linear correlation. Moreover, higher hydrogen concentrations shift the peak flame temperature upstream, with its position moving from 0.046 to 0.026 m on the axial line.

3.3. Effect of Hydrogen Blending Ratio in the Inlet Mixture on Reaction Chemical Structure in the Burner.

The hydrogen blending to LFG30 alters the chemical reactions in the combustion zone and the resulting intermediate species.

https://doi.org/10.1021/acsomega.5c05809
ACS Omega 2025, 10, 41809−41819

To study these variations and the effect on combustion performance, mole fractions of different species were analyzed for the combustion of LFG30 with and without hydrogen blending. In this analysis, the concentrations of carbon-containing species were normalized, with respect to the initial amount of carbon introduced into the system. Figure 8

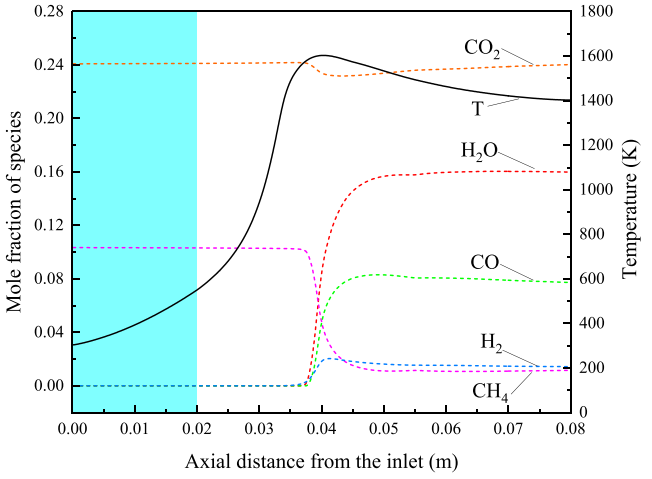

Figure 8. Chemical reaction structure for combustion of pure LFG30 at flow velocity, u_{in} = 0.15 m/s and Φ = 1.5.

illustrates the axial temperature distribution and the distribution of the key species for pure LFG30. It can be observed that the temperature gradually increases from the burner inlet, while the mole fractions of the species in the mixture remain relatively unchanged at the initial stage, indicating the absence of combustion reactions. When the temperature reaches approximately 800 K, the mole fraction of methane (CH_4) starts to decrease rapidly, while the mole fractions of products such as CO and H_2O begin to increase steadily, signifying the onset of combustion reactions. This suggests that the initial temperature increase is primarily caused by heat transfer from the high-temperature downstream region through the porous medium, which preheats the incoming gas mixture. The preheating process enables methane to rapidly reach its ignition temperature, triggering intense chemical reactions and causing a sharp increase in the burner's internal temperature. During this phase, the temperature gradient reaches its maximum value.

Figure 9 shows the axial temperature and species concentration profiles when the hydrogen concentration in the inlet mixture is 20%. Compared to the pure LFG30 case, the flame front shifts significantly toward the burner inlet. From x = 0.015−0.025 m, the mole fractions of CH_4 and H_2 decrease sharply, accompanied by a rapid rise in temperature. The upstream movement of the flame front also causes the high-gradient region (characterized by steep changes in temperature and species concentrations) to shift closer to the burner inlet. Furthermore, the mole fractions of CO and CO_2 are significantly reduced compared with pure LFG30.

3.4. Effect of Hydrogen Blending Ratio in the Inlet Mixture on CO and NO_x Emissions. The axial distributions of CO and NO_x along the burner were analyzed, as illustrated in Figure 10. In the simulation, the radical species critical for thermal-NO_x formation are directly handled by the use of a standard thermal-NO_x estimation model (Zeldovich mechanism) integrated with ANSYS Fluent. The Partial Equilibrium

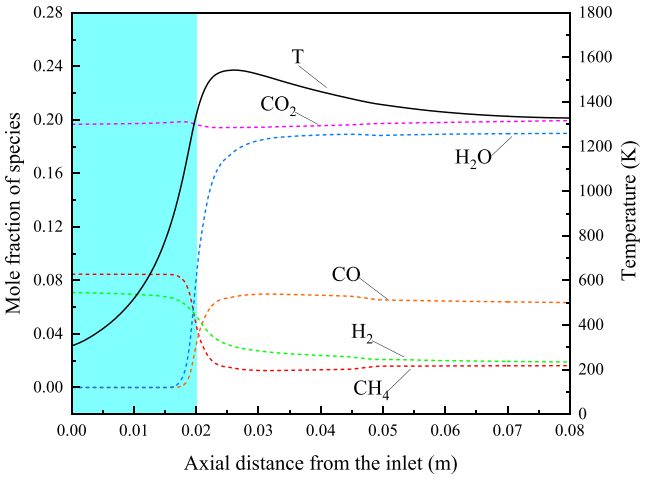

Figure 9. Chemical reaction structure for combustion of LFG30 with 20% hydrogen at flow velocity, u_{in} = 0.15 m/s and Φ = 1.5.

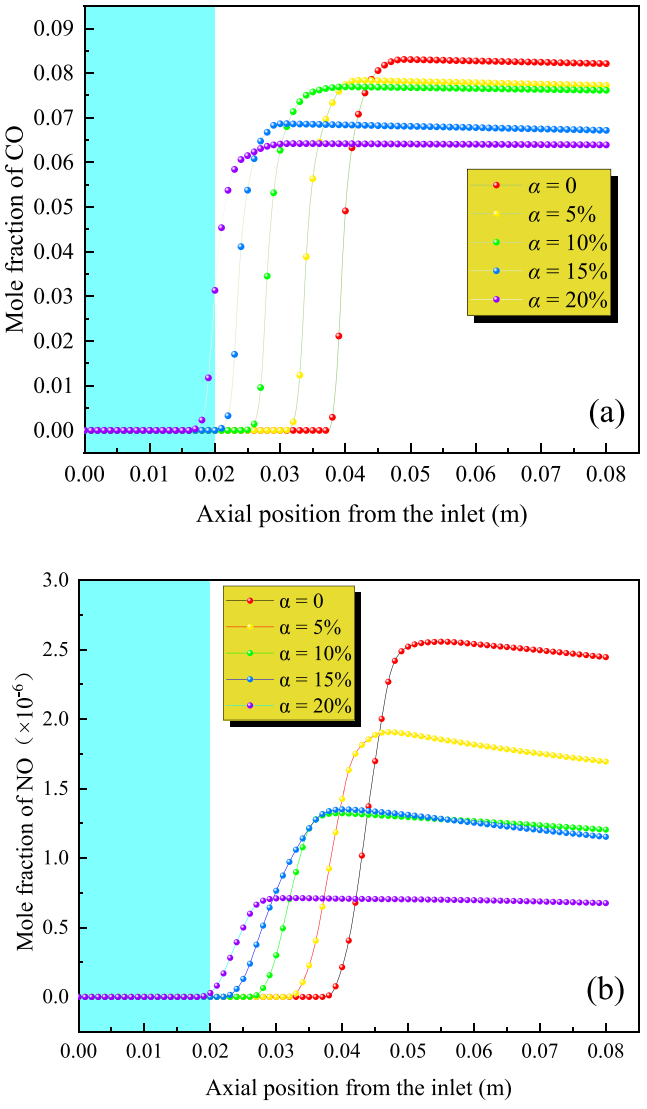

Figure 10. CO and NO_x distribution for different hydrogen blending ratios at flow velocity, u_{in} = 0.15 m/s and Φ = 1.5; (a) mole fraction of CO; (b) mole fraction of NO_x.

https://doi.org/10.1021/acsomega.5c05809
ACS Omega 2025, 10, 41809−41819

assumption was applied to approximate the OH concentration. Given the inherent limitations of the NO_x estimation methodology employed in this study, the resulting data are presented solely for comparative analysis. Simulation results indicate noticeable changes in the CO and NO_x mole fractions as the hydrogen blending ratio increased. The positions of the steep gradients align with the flame front, indicating that CO and NO_x are primarily produced within the main reaction zone of combustion. Furthermore, a higher hydrogen content significantly reduces the CO and NO_x concentrations in the reaction zone. Both species reach peak concentrations at the flame front and then slightly decrease due to subsequent branching reactions. The conversion of CO to CO_2 is closely related to the reaction between CO and OH radicals formed during the combustion process, specifically through reaction pathway R13: CO + OH → CO_2 + H. According to the sensitivity analysis performed (see Figure 12), when more hydrogen is blended with the fuel, the conversion of CO to CO_2 via reaction R13 accelerates, thereby reducing CO emissions. As shown in Figures 6 and 7, a higher H_2 fraction results in a lower peak temperature within the burner. This temperature reduction subsequently decreases the level of formation of thermal-NO_x, leading to reduced NO_x emissions.

To accurately assess the impact of the hydrogen blending ratio on CO and NO_x emissions, the spatially averaged mole fractions (normalized to 3.5% O_2) at the burner outlet are presented in Figure 11. Both the CO and NO_x concentrations

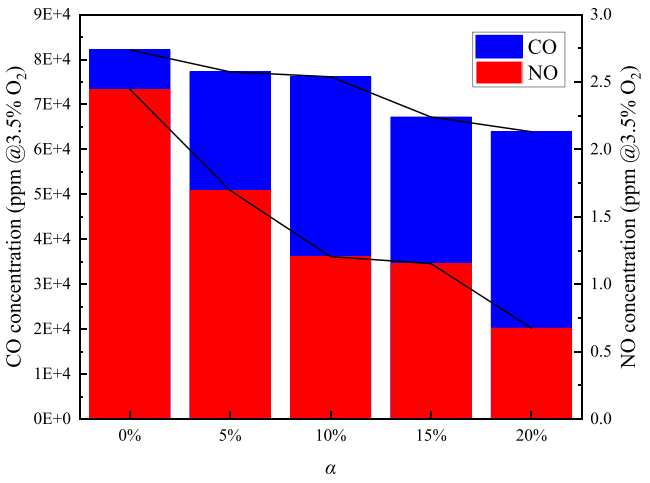

Figure 11. Average CO and NO_x emissions at outlet with different hydrogen blending ratios at flow velocity, u_{in} = 0.15 m/s and Φ = 1.5.

exhibit a declining trend with increasing hydrogen fraction. When the hydrogen blending ratio increases from 0 to 20%, the exit mole fractions of CO and NO_x decrease by 22.14 and 72.65%, respectively. This indicates that the addition of hydrogen effectively mitigates pollutant emissions. Notably, CO emission is substantially high due to incomplete combustion associated with the use of a rich fuel mixture where Φ = 1.5. In contrast, NO_x emissions remain low, reflecting the low-NO_x characteristic of porous media combustion. This is because NO_x generation in the burner is primarily influenced by thermal-NO_x and prompt-NO_x mechanisms: (1) Elevated hydrogen blending lowers local flame temperatures, suppressing thermal-NO_x formation; (2) The low methane content in the low-calorific landfill gas provides insufficient CH radicals for prompt-NO_x production.

3.5. Effect of Hydrogen Blending Ratios in the Inlet Mixture on Combustion Process. The primary combustible component of LFG is methane. The combustion process of methane involves a chain reaction composed of multiple branching reactions. The addition of hydrogen introduces new branching reaction pathways into the methane combustion process. This significantly affects the combustion characteristics of LFG, including the temperature distribution, species concentration, reaction rates, and reaction zones during combustion. This phenomenon is closely related to the unique thermophysical properties of hydrogen. Moreover, the intrinsic chain reactions of hydrogen further interact with methane combustion reactions, altering the chemical kinetics of the process. Therefore, to better understand the impact of hydrogen addition on the key chemical reactions in LFG combustion, sensitivity analysis was performed.

The normalized sensitivity coefficients for different reaction pathways were calculated for hydrogen mole fractions ranging from α = 0 to 20%, as shown in Figure 12. The intensity of the combustion reactions is closely related to the concentration of highly reactive radicals, such as H, OH, and O, in the radical pool. These radicals play a crucial role as both reactants and products in chain branching reactions, and they are eventually consumed in chain termination reactions, forming stable products such as H_2O and CO_2. Figure 12 shows that the positive sensitivity coefficients of the chain branching reactions R1: H + O_2 ⇌ OH + O and R30: CH_3 + HO_2 ⇌ CH_3O + OH gradually decrease with the hydrogen mole fraction. This reduction in OH radical formation has an effect on further chain branching reactions, and it explains the reason for the relative reduction of overall burner temperature with the addition of hydrogen. The sensitivity coefficient of OH-consuming reaction R13: CO + OH ⇌ CO_2 + H increases with the addition of hydrogen. It converts CO to CO_2 and reduces the overall CO emission.

Overall, as the hydrogen blending ratio (α) increases, both the positive and negative sensitivity coefficients exhibit varying degrees of change. This is primarily due to the significant impact of hydrogen addition on the production and consumption of key radicals (H, OH, and O), which subsequently alter the flame's heat release characteristics and chemical reaction structure.

4. CONCLUSIONS

This study investigated the effects of hydrogen addition on the combustion characteristics of low-calorific-value landfill gas under fuel-rich conditions in a double-layer porous media burner using numerical simulations. The key findings are summarized as follows:

1. Hydrogen blending in LFG30 significantly broadens the stable combustion range in double-layer porous media burners. The observed asymmetric widening of the stable combustion range is attributed to hydrogen's high thermal diffusivity, which enhances upstream heat recirculation. This notably increases the upper blow-off limit while the lower flashback limit remains largely unchanged. The expanded stable combustion range enhances operational flexibility of combustion systems utilizing hydrogen-enriched low-calorific-value LFG.
2. With the increase in hydrogen blending ratio in the mixture, the flame zone shifts upstream, and the combustion temperature slightly decreases. This results

https://doi.org/10.1021/acsomega.5c05809
ACS Omega 2025, 10, 41809−41819

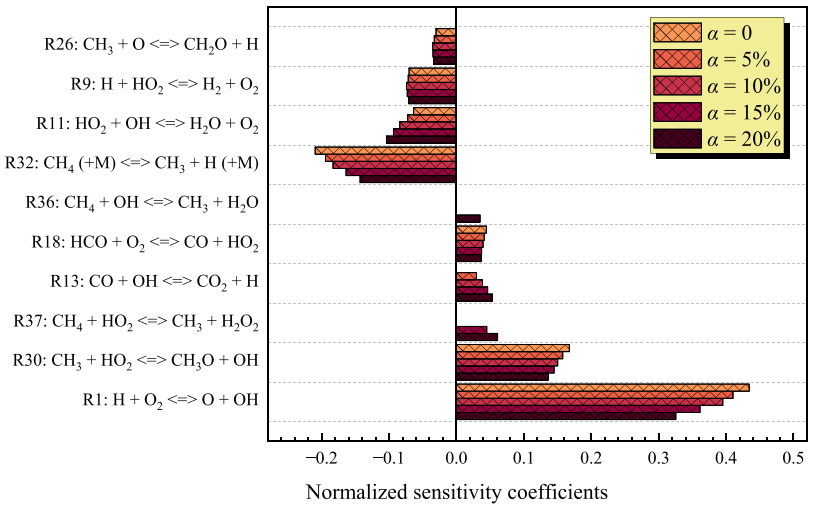

Figure 12. Normalized sensitivity coefficients of significant reaction pathways at different hydrogen blending ratios in the fuel mixture at flow velocity, u_{in} = 0.15m/s and Φ = 1.5.

in a decrease in exhaust gas temperature. Furthermore, higher hydrogen concentration leads to a reduction in peak combustion temperature and shifts the location of the peak temperature toward the upstream region.

3. The concentration profiles of CO and NO_x within the burner show no significant differences between the combustion of pure LFG30 and hydrogen-enriched LFG30. However, when the hydrogen blending ratio reaches 20%, the mole fractions of CO and NO_x at the outlet decrease by 22.14 and 72.65%, respectively, compared to the pure LFG30. This indicates that hydrogen addition effectively reduces CO and NO_x emissions from low-calorific LFG combustion.
4. As the hydrogen blending ratio increases, the positive sensitivity coefficient of the exothermic reaction R1: H + O_2 ⇌ OH + O decreases, resulting in a lower overall heat release. This change is a contributing factor to the observed reduction in burner temperature with higher hydrogen blending ratios. Additionally, Reaction R13: CO + OH ⇌ CO_2 + H plays a significant role in facilitating the conversion of CO to CO_2 at elevated hydrogen concentrations.

While this study provides valuable insights toward developing practical porous media burners for combustion of H_2-enriched low-calorific LFG, several limitations should be acknowledged. The model assumes adiabatic burner walls, which means it does not account for heat losses that commonly occur in practical burner operations. Future research should therefore investigate the effects of heat losses on combustion characteristics to improve the reliability of numerical predictions. Additionally, the current analysis focuses solely on the combined effect of porous media combustion and H_2 enrichment in low-calorific LFG. Other potentially influential factors, such as the interplay between hydrogen diffusivity and the thermal conductivity of the porous medium, have not been fully explored and warrant further study.

AUTHOR INFORMATION

Corresponding Author

Udaya Kahangamage − *Division of Science, Engineering and Health Studies, School of Professional Education and Executive Development, The Hong Kong Polytechnic University, Kowloon 999077, Hong Kong;* orcid.org/0000-0001-9009-5151; Email: udaya.kahangamage@cpce-polyu.edu.hk

Authors

Kang Tan − *Division of Science, Engineering and Health Studies, School of Professional Education and Executive Development, The Hong Kong Polytechnic University, Kowloon 999077, Hong Kong*

Kangdong Chen − *Division of Science, Engineering and Health Studies, School of Professional Education and Executive Development, The Hong Kong Polytechnic University, Kowloon 999077, Hong Kong*

Chun-wah Leung − *Division of Science, Engineering and Health Studies, School of Professional Education and Executive Development, The Hong Kong Polytechnic University, Kowloon 999077, Hong Kong*

Complete contact information is available at: https://pubs.acs.org/10.1021/acsomega.5c05809

Notes

The authors declare no competing financial interest.

ACKNOWLEDGMENTS

The work described in this paper was fully supported by a grant from the Research Grants Council of the Hong Kong Special Administrative Region, China (UGC/FDS24/E07/23).

NOMENCLATURE

LFG	landfill gas
x	x-direction position, m
y	y-direction position, m
ρ_g	density of the fuel/air mixture, kg/m^3
ϵ	porosity of the porous medium
d_p	pore size of porous medium, mm
Φ	fuel/air mixture equivalence ratio
u_{in}	inlet flow velocity, m/s
u	velocity in x-direction, m/s
$\vec{u}$	x-direction velocity vector
v	velocity in y-direction, m/s

https://doi.org/10.1021/acsomega.5c05809
ACS Omega 2025, 10, 41809−41819

$\vec{v}$ y-direction velocity vector
ω_i molar yield of substance i
Y_i local mass fraction of species i
M_i molecular weight of component i, kg/mol
D_{in} mass diffusion coefficient of species i, m^2/s
$\overline{W}$ mean molecular weight of the fuel/air mixture, g/mol
α mole fraction of hydrogen in the fuel mixture, %
C_1 viscous resistance coefficient, $1/m^2$
C_2 inertial resistance coefficient, 1/m
λ_{eff} effective thermal conductivity of the porous medium, W/(m·K)
λ_g thermal conductivity of the gas phase, W/(m·K)
λ_s thermal conductivity of the solid phase, W/(m·K)
n_{H_2} mole fraction of hydrogen in the fuel mixture
n_{LFG} mole fraction of landfill gas in the fuel mixture
T_{outlet} burner outlet temperature, K
T_{peak} burner peak temperature, K
x_{peak} axial position of peak temperature, m

REFERENCES

(1) Hoang, A. T.; Pham, V. V.; Nguyen, X. P. Integrating renewable sources into energy system for smart city as a sagacious strategy towards clean and sustainable process. *J. Cleaner Prod.* **2021**, *305*, No. 127161.
(2) Nam, H. T.; Jeon, Y.; Lee, S.; Jung, H. Experimental study on combustion and thermal characteristics of impinging premixed flames for low heating value gas (LHVG) fuels. *Case Stud. Therm. Eng.* **2023**, *47*, No. 103032.
(3) Ayodele, T. R.; Alao, M. A.; Ogunjuyigbe, A. S. O. Effect of collection efficiency and oxidation factor on greenhouse gas emission and life cycle cost of landfill distributed energy generation. *Sustainable Cities Soc.* **2020**, *52*, No. 101821.
(4) Melikoglu, M. Vision 2023: Assessing the feasibility of electricity and biogas production from municipal solid waste in Turkey. *Renewable Sustainable Energy Rev.* **2013**, *19*, 52−63.
(5) Zuberi, M. J. S.; Ali, S. F. Greenhouse effect reduction by recovering energy from waste landfills in Pakistan. *Renewable Sustainable Energy Rev.* **2015**, *44*, 117−131.
(6) Kahangamage, U.; Chen, K.; Zhen, H.; Leung, C.-w. Numerical investigation of combustion characteristics of hydrogen-enriched low calorific value landfill gas for energy applications. *Energy Rep.* **2024**, *12*, 173−186.
(7) Buckmaster, J. Stability of the porous plug burner flame. *SIAM J. Appl. Math.* **1983**, *43* (6), 1335−1349.
(8) Gharehghani, A.; Ghasemi, K.; Siavashi, M.; Mehranfar, S. Applications of porous materials in combustion systems: A comprehensive and state-of-the-art review. *Fuel* **2021**, *304*, No. 121411.
(9) Wu, C.-Y.; Chen, K.-H.; Yang, S. Y. Experimental study of porous metal burners for domestic stove applications. *Energy Convers. Manage.* **2014**, *77*, 380−388.
(10) Wei, D.; Peng, Q.; Yin, R.; et al. Optimizing micro power generation with blended fuels and porous media for H2-fueled combustion. *Renewable Energy* **2024**, *233*, No. 121188.
(11) Saravanan, S.; Ramesh Kumar, C.; Pugazhendhi, A.; Brindhadevi, K. Role of thermal barrier coating and porous medium combustor for a diesel engine: An experimental study. *Fuel* **2020**, *280*, No. 118597.
(12) Howell, J. R.; Hall, M. J.; Ellzey, J. L. Combustion of hydrocarbon fuels within porous inert media. *Prog. Energy Combust. Sci.* **1996**, *22* (2), 121−145.
(13) Al-Hamamre, Z.; Diezinger, S.; Talukdar, P.; Von Issendorff, F.; Trimis, D. Combustion of Low Calorific Gases from Landfills and Waste Pyrolysis Using Porous Medium Burner Technology. *Process Saf. Environ. Prot.* **2006**, *84* (4), 297−308.
(14) Chen, Y.; Long, L.; Hu, J.; et al. The combustion characteristics and stable limit of a novel combustor with gradient porous media for hydrogen-enriched natural gas. *J. Energy Inst.* **2024**, *116*, No. 101743.
(15) Bubnovich, V.; Hernandez, H.; Toledo, M.; Flores, C. Experimental investigation of flame stability in the premixed propane-air combustion in two-section porous media burner. *Fuel (Guildford)* **2021**, *291*, No. 120117.
(16) Dai, H.; Zhang, B.; Li, Z.; Wu, J. Combustion characteristics of a porous media burner with partial hydrogen injection. *Int. J. Hydrogen Energy* **2022**, *47* (2), 1092−1102.
(17) Alavandi, S. K.; Agrawal, A. K. Experimental study of combustion of hydrogen−syngas/methane fuel mixtures in a porous burner. *Int. J. Hydrogen Energy* **2008**, *33* (4), 1407−1415.
(18) Devi, S.; Sahoo, N.; Muthukumar, P. Experimental studies on biogas combustion in a novel double layer inert Porous Radiant Burner. *Renewable Energy* **2020**, *149*, 1040−1052.
(19) Bubnovich, V.; Hernandez, H.; Toledo, M.; Flores, C. Experimental investigation of flame stability in the premixed propane-air combustion in two-section porous media burner. *Fuel* **2021**, *291*, No. 120117.
(20) Habib, R.; Yadollahi, B.; Saeed, A.; Doranehgard, M. H.; Karimi, N. On the Response of Ultralean Combustion of CH4/H2 Blends in a Porous Burner to Fluctuations in Fuel Flow—an Experimental Investigation. *Energy Fuels* **2021**, *35* (10), 8909−8921.
(21) Keramiotis, C.; Founti, M. A. An experimental investigation of stability and operation of a biogas fueled porous burner. *Fuel* **2013**, *103*, 278−284.
(22) Chen, K.; Kahangamage, U.; Tan, K.; Leung, C.-W. Heat transfer analysis of premixed low calorific value landfill gas impinging flame under oxygen and hydrogen enrichment. *Results Eng.* **2025**, *25*, No. 104118.
(23) Francisco, R. W., Jr; Costa, M.; Catapan, R. C.; Oliveira, A. A. M. Combustion of hydrogen rich gaseous fuels with low calorific value in a porous burner placed in a confined heated environment. *Exp. Therm. Fluid Sci.* **2013**, *45*, 102−109.
(24) Amez, I.; Castells, B.; Ortega, M. F.; Llamas, B.; García-Torrent, J. Experimental study of flame zones variations of biogas enriched with hydrogen. *Int. J. Hydrogen Energy* **2022**, *47* (57), 24212−24222.
(25) Chen, Y.; Long, L.; Niu, J.; et al. Investigation on the Combustion Characteristics and Environmental Effects of Hydrogen-doped Natural Gas for Domestic Water Heaters. *ACS Omega* **2023**, *8* (50), 48370−48380.
(26) Tolouei, A.; Gharehghani, A. Effect of hydrogen enrichment and catalytic porous media on the combustion characteristics of methane/ammonia. *Int. J. Hydrogen Energy* **2025**, *146*, No. 149986.
(27) Wang, Y.; Zeng, H.; Shi, Y.; Cai, N. Methane partial oxidation in a two-layer porous media burner with Al2O3 pellets of different diameters. *Fuel* **2018**, *217*, 45−50.
(28) Yang, W.; Wang, Y.; Zhou, J.; Yao, Y.; Zhu, X.; Cen, K. Simulation of hetero/homogeneous combustion characteristics of CH4/air in a half packed-bed catalytic combustor. *Chem. Eng. Sci.* **2020**, *211*, No. 115247.
(29) Oberkampf, W. L.; Trucano, T. G. Verification and validation in computational fluid dynamics. *Prog. Aeronaut. Sci.* **2002**, *38* (3), 209−272.
(30) Turkeli-Ramadan, Z.; Sharma, R. N.; Raine, R. R. Two-dimensional simulation of premixed laminar flame at microscale. *Chem. Eng. Sci.* **2015**, *138*, 414−431.
(31) Zhang, Z.; Ye, J.; Tan, D.; et al. The effects of Fe2O3 based DOC and SCR catalyst on the combustion and emission characteristics of a diesel engine fueled with biodiesel. *Fuel* **2021**, *290*, No. 120039.
(32) Mohammadi, I.; Ajam, H. A theoretical study of entropy generation of the combustion phenomenon in the porous medium burner. *Energy* **2019**, *188*, No. 116004.
(33) Zeng, H.; Wang, Y.; Shi, Y.; Ni, M.; Cai, N. Syngas production from CO2/CH4 rich combustion in a porous media burner:

https://doi.org/10.1021/acsomega.5c05809
ACS Omega 2025, 10, 41809−41819

Experimental characterization and elementary reaction model. *Fuel* **2017**, *199*, 413−419.
(34) Omar, H. M.; Rohani, S. Removal of CO2 from landfill gas with landfill leachate using absorption process. *Int. J. Greenhouse Gas Control* **2017**, *58*, 159−168.
(35) Fruzza, F.; Chu, H.; Lamioni, R.; Grenga, T.; Galletti, C.; Pitsch, H. Three-dimensional numerical investigation of flashback in premixed hydrogen flames within perforated burners. *Combust. Flame* **2025**, *274*, No. 113987.

https://doi.org/10.1021/acsomega.5c05809
ACS Omega 2025, 10, 41809−41819